An expanded palette of fluorogenic HaloTag probes with enhanced contrast for targeted cellular imaging

Sylvestre P.J.T. Bachollet,[a] Yuriy Shpinov,[a] Fanny Broch,[a] Hela Benaissa,[a] Arnaud Gautier,[a,b] Jean-Maurice Mallet[a] and Blaise Dumat[a]*

[a] Laboratoire des biomolécules, LBM, Département de chimie, École normale supérieure, PSL University, Sorbonne Université, CNRS, 75005 Paris, France.
[b] Institut Universitaire de France (IUF), 1 rue Descartes, 75005 Paris

*Corresponding author : blaise.dumat@ens.psl.eu

Introduction

Fluorescence imaging has become an invaluable tool to study the structure and dynamics of living systems due to its high sensitivity (down to the single molecule), high temporal and spatial resolution and to its biocompatibility, allowing non-invasive imaging of samples in physiological conditions. Numerous fluorescent molecular probes have been developed over time and organic chemistry offers virtually endless possibilities to tailor fluorophores for each application.[1] Nonetheless, since the discovery of the Green Fluorescent Protein (GFP), fluorescent proteins (FPs) have taken a prominent place in the field of bioimaging thanks to the unparalleled targeting selectivity of genetic encoding. A large variety of FPs has since been developed with emission spanning the whole visible spectrum and optimized optical and biochemical properties paving the way to multicolor and complex imaging experiments.[2] More recently, hybrid chemogenetic systems have appeared, that associate a genetically encoded self-labeling protein tag with a small molecular fluorophore linked either covalently or non-covalently to the protein.[3–7] Such combination benefits from the genetic targeting of FPs and from the structural diversity and versatility of organic chromophores and it offers better spatial and temporal control over the fluorescent labeling compared to fluorescent proteins that are continuously expressed and fluorescent. It may nonetheless suffer from common problems associated with molecular probes, including the risk of off-target binding, yielding non-specific signal, and the need to wash the excess of dye. To alleviate these issues, advanced chemogenetic reporters are built on fluorogenic probes that only become fluorescent when bound to the cognate protein tags.[8–11] Considerable efforts have thus been put in the development of fluorogens with diverse optical properties and on their association with protein tags, in particular the most commonly used SNAP-tag[12–15] and HaloTag.[16–21] The latter is, to date, one the most useful tag for covalent protein labeling with high selectivity and fast reaction kinetics. Its chemically simple and lipophilic chloroalkane ligand also facilitates the synthesis of the dedicated probes as well as their cell permeability.[22]

The HaloTag is derived from a bacterial alkane dehalogenase and was built and optimized (up to the last iteration HaloTag7) to bind xanthene dyes and especially rhodamine derivatives with high reaction rates (k_2 = 1.9 x 10^7 M^{-1}s^{-1} for TMR-Halo at 25°C).[3,23] This has driven a lot of the research on HaloTag probes towards rhodamines and, more particularly, fluorogenic Si-Rhodamines taking advantage of the polarity-sensitive spirocyclization reaction.[19,20,22,24–26] This approach certainly yields highly efficient fluorescent chemogenetic reporters but has narrowed their chemical diversity. Alternative strategies to develop fluorogenic HaloTag probes have relied on the intrinsic viscosity and/or polarity-sensitive emission of dipolar fluorophores.[16,17,27] The approach was pioneered by Kool and coworkers who developed a dimethylamino-styrylpyridinium dye with a viscosity-sensitive emission that was activated upon reaction with HaloTag thanks to the immobilization inside the protein binding pocket. This so-called "molecular rotor" design allows exploring a much wider chemical space: the fluorescence activation mechanism is applicable to a large variety of dipolar structures with electron-donating and withdrawing groups connected through a flexible conjugated bond and is commonly used to develop biomolecular probes.[28–33] Based on this strategy, we have previously designed a series of red and far-red emitting fluorogenic HaloTag probes (Figure 1A).[21] After reaction with HaloTag, the probes are covalently tethered to the protein and exhibit large enhancements of their fluorescence emissions compared to their free form in water

(up to 156-fold). The two most promising fluorogens **Red-Halo2** and **NIR-Halo1** enabled wash-free imaging of the nucleus and actin in live cells by targeting HaloTag-NLS and HaloTag-LifeAct fusion proteins respectively. We nonetheless observed a low nonspecific signal in the cytoplasm that may prove detrimental when imaging low-abundant or cytosolic proteins.

Herein, taking advantage of the versatile design, we report an expanded palette of HaloTag fluorogens designed to cover a wider emission range from green to red and to minimize the non-specific signal. The new set of probes was characterized in vitro by absorption and fluorescence spectroscopies and in cell imaging by confocal microscopies. Some new analyses were also performed on the previously reported **Red-Halo2** and **NIR-Halo1** probes for comparison purposes. The photophysical properties were studied *in vitro* in glycerol and in presence of HaloTag to confirm their viscosity-dependent emission and fluorogenic reaction with the protein tag. The selectivity of the probes in wash-free imaging experiments was then studied in cells and, taking advantage of the superior contrast of the newly designed probes, we applied them to image of a variety of cellular organelles and proteins.

Results and discussion

Design and synthesis. The previously reported Red-Halo and NIR-Halo probes cover an emissive range from red to far-red. In order to cover a lower wavelength range, we have modified **Red-Halo2** to introduce two lesser deficient electron-withdrawing groups, 2-cyanoacetic acid or imidazolinone, to form, respectively, two green and yellow emitting derivatives **CCVJ-Halo** and **Y-Halo**. 2-Cyanoacetic acid forms the CCVJ fluorophore which is a classical molecular rotor with a green emission used as a fluorogenic protein probe and it presents a readily available carboxylic acid function for conjugation with the HaloTag ligand.[13,34,35] CCVJ was already used with HaloTag but with a different ligand unit which does not readily make the probe fluorogenic upon reaction with the protein and was instead used to detect protein aggregation.[27] Imidazolinone on the other hand is the electron withdrawing group found in the GFP chromophore and, in aminated derivatives, it was reported to afford yellow-emitting compounds.[36]
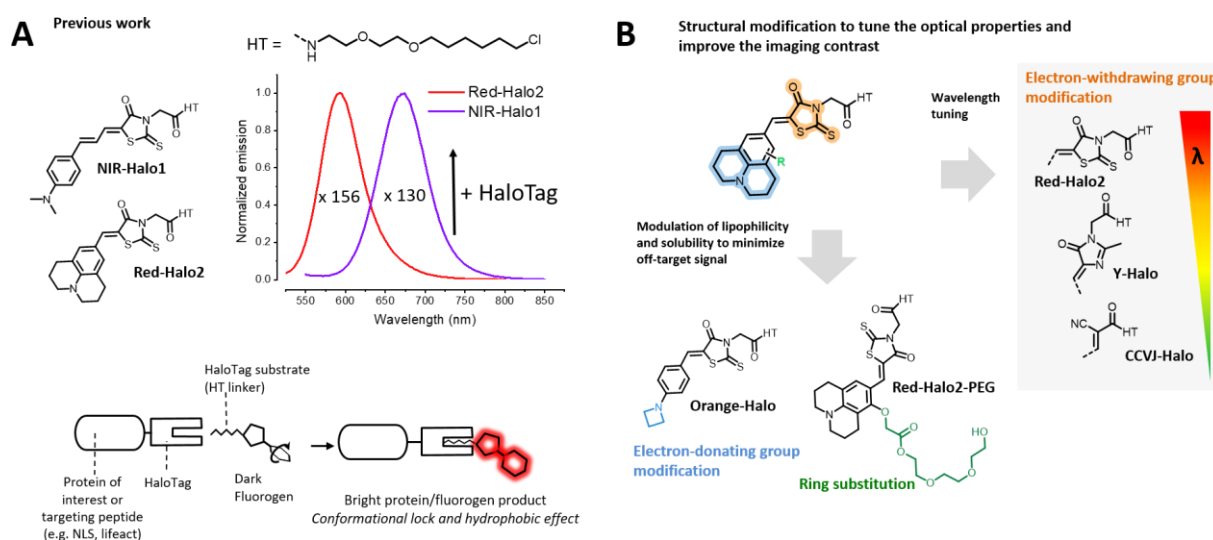

Figure 1. Design and structures of the fluorogenic HaloTag probes.
(A) structures of two of the previously reported probes with their fluorescence emission spectra and fluorescence enhancement upon reaction with HaloTag and general schematic description of the fluorogenic reaction with HaloTag. (B) Structural modifications and structures of the new probes.

In order to minimize the unspecific signal observed with **Red-Halo2** and **NIR-Halo1**, we have set out to develop analogs with similar optical properties as **Red-Halo2** but with lower lipophilicity. Factors governing the non-specific binding of a dye to intracellular components are difficult to predict and depend in part on the net charge (*e.g.* positively charged rhodamine binding to mitochondria) and on the lipophilic/hydrophilic balance. The Halo

dyes being neutral structures with poor water solubility, we hypothesized that their lipophilic character is one of the driving force of the non-specific binding by leading the probes to accumulate into lipid structures such as the endoplasmic reticulum (ER) membrane. As a first strategy, we have synthesized **Red-Halo2-PEG** with a similar core structure than **Red-Halo2** but bearing a solubilizing triethylene glycol chain on the aniline ring. In a second approach, we have introduced an azetidine donating amino group instead of the julolidine (Figure 1). Azetidine was previously reported as an efficient locked amino donating group since the 4-membered cycle strain prevents the formation of a "twisted intramolecular charge transfer" (TICT) state and it may advantageously replace julolidine while being slightly less lipophilic.[20] Azetidine is also less electron-donating than julolidine and yielded the blue-shifted orange-emitting **Orange-Halo**. Using inexpensive building blocks and reagents, the probes can be obtained in straightforward 2 to 4 steps synthetic procedures detailed in the supplementary information (Scheme S1-S4).

Photophysical characterization in glycerol. All probes display typical molecular rotor features, with a donor and acceptor group connected through a flexible bond, and we have previously evidenced the fluorogenic behavior of **Red-Halo2** and **NIR-Halo1** in presence of proteins while CCVJ is an archetypical rotor probe. We have nonetheless confirmed the molecular rotor properties (*i.e.* the viscosity-dependent emission) for the whole series of probes by measuring their spectral properties in water and in glycerol (Figure 2 and Table 1).
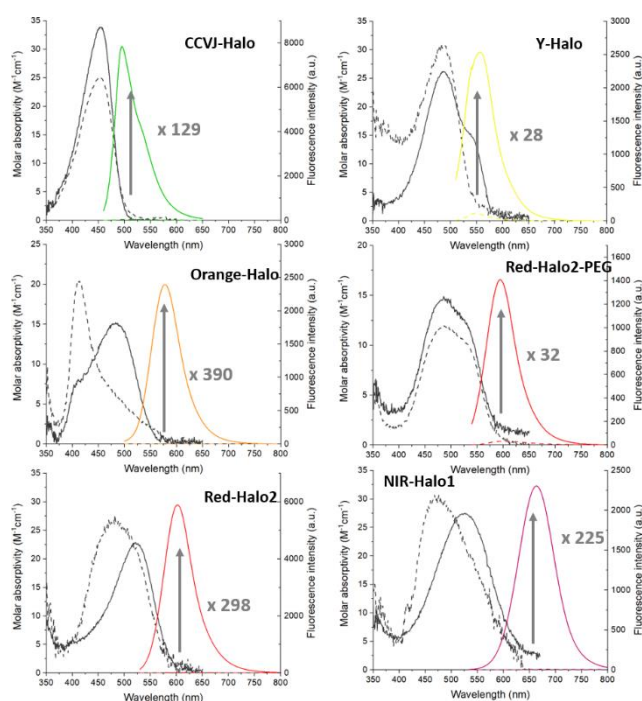

Figure 2. Viscosity-dependent emission of the molecular rotor probes.
Absorption (black lines) and fluorescence emission (colored lines) in water (dashed lines) and in glycerol (full lines) of the Halo probes. On each panel is also indicated the fluorescence enhancement factor F/F_0 where F is the fluorescence intensity in glycerol and F_0 the fluorescence in water.

As expected from the rational design, all probes are weakly fluorescent in water but their emission is strongly enhanced in glycerol with quantum yields ranging from 9 to 20 %, in accordance with an increase in viscosity. The highest brightness in glycerol is observed for **CCVJ-Halo** with a 129-fold enhancement and a green emission centered on 495 nm, which confirms that CCVJ conjugated to the HaloTag ligand retains its molecular rotor properties. **Y-Halo** exhibits a slightly higher residual fluorescence in water as well as a lower brightness in glycerol which results in a lower flurogenicity. Although the azetidine is slightly less electron-donating than the julolidine, **Orange-Halo** is expected to have spectral properties close to those of **Red-Halo2** but its absorption in water is unexpectedly blue-shifted (409 nm). In glycerol however, a large bathochromic shift is observed resulting in an absorption spectrum more akin to the parent **Red-Halo2** structure with a corresponding emission centered on

578 nm, blue-shifted by 24 nm compared to **Red-Halo2**. The activation of the fluorescence in glycerol combined with the shift of the excitation maximum result in the highest enhancement of the series (390-fold), although the brightness remains lower than that of CCVJ-Halo. **Red-Halo2** and **NIR-Halo1** exhibit similar behaviors as were observed in presence of HaloTag with a red-shift of the absorption between water and glycerol and a large fluorescent enhancement of their red and far-red emission centered on 602 and 664 nm respectively.[21] The spectral properties of **Red-Halo2-PEG** are essentially conserved compared to its parent compound but its brightness is significantly lower resulting in a lower fluorogenicity.

Table 1. Photophysical properties in Glycerol

maximum absorption wavelength λ_{abs}; molar absorptivity ε; maximum emission wavelength λ_{em}; fluorescence quantum yield Φ_F; emission brightness $\varepsilon \cdot \Phi_F$; fluorescence enhancement between water and glycerol F/F_0 where F is the fluorescence in glycerol and F_0 the fluorescence in water measured at a 2 µM concentration in dye.

	λ_{abs} (nm)	ε ($M^{-1}cm^{-1}$)	λ_{em} (nm)	Φ_F	$\varepsilon \cdot \Phi_F$	F/F_0
CCVJ-Halo	455	33900	495	0.19	6441	129
Y-Halo	487	26200	556	0.099	2594	28
Orange-Halo	486	15200	578	0.14	2128	390
Red-Halo2-PEG	520	14900	595	0.086	1281	32
Red-Halo2	521	22900	602	0.20	4580	298
NIR-Halo1	527	27500	664	0.091	2503	225

Reaction with HaloTag and photophysical properties. The properties in glycerol confirm the potential of the probes to be used as fluorogenic biomolecular probes thanks to a viscosity-sensitive emission and we next studied the reaction of the probes with a GST-HaloTag (GST-HT) protein *in vitro* and the resulting fluorescence properties of the formed complexes. The results are summarized in table 2 and Figure 3.

Table 2. Photophysical properties of the dyes bound to GST-HaloTag.

λ_{abs} and λ_{em}: maximum absorption and emission wavelength, ε: molar absorptivity coefficient, *FWHM*: Full width at Half maximum, Φ_F: fluorescence quantum yield, $\varepsilon \cdot \Phi_F$: brightness, k_2: second order reaction rate constant, F/F_0: Fluorescence enhancement factor where F and F_0 are the integrated fluorescence intensities in presence of HaloTag and in water respectively.

	λ_{abs} (nm)	ε ($10^3 M^{-1}cm^{-1}$)	λ_{em} (nm)	FWHM (nm)	Φ_F	$\varepsilon \cdot \Phi_F$	k_2^b ($10^3 M^{-1}s^{-1}$)	F/F_0
CCVJ-Halo	458	31.8	498	54	0.014	445	1.0 ± 0.1	15
Y-Halo	489	34.9	562	50	0.015	524	n.d.	12
Orange-Halo	487	16.2	574	64	0.02	324	0.45 ± 0.03	48
Red-Halo2-PEG	504	14.5	588	65	0.05	725	0.29 ± 0.04	32
Red-Halo2[a]	515	21.0	592	60	0.17	3600	1.3 ± 0.2	156
NIR-Halo1[a]	526	25.8	671	68	0.053	1400	1.7 ± 0.04	130

Measurement conditions: 1 µM dye with 1.7 µM GST-HT in pH 7.4 phosphate buffer containing 10 mM Phosphate and 100 mM NaCl. [a] Data taken from ref. [21] except for k_2 values. [b] Average of duplicate experiments.

All probes undergo a fluorogenic reaction reaction with GST-HT, which allowed us to measure the reaction rate constants by following the increase of fluorescence over time (Figure 3A&B). In presence of a large excess of protein, the reactions obey a classical pseudo-first-order exponential law with the exception of **Y-Halo** and the calculated second order reaction rate constants are comprised between 0.29×10^3 and 1.7×10^3 $M^{-1}s^{-1}$. The slowest reaction rates were observed for **Orange-Halo** and **Red-Halo2-PEG** which can be explained in part by solubility and steric hindrance issues. The unexpectedly blue-shifted absorption of **Orange-Halo** suggests the formation of aggregates which may also explain the slow reaction kinetics and **Red-Halo2-PEG** bears a PEG chain that may hinder the reaction. On the other hand, the fastest reaction rate is observed for **NIR-Halo1** in which the extended π-system takes the bulky aromatic group further from the reaction site. The reaction with **Y-Halo** is almost instantaneous with an immediate sharp increase of fluorescence that is followed by a slower decrease of intensity that stabilizes after a few minutes (Figure 3B). It is possible that **Y-Halo** undergoes a first non-covalent association with the protein yielding a highly fluorescent complex followed by the covalent enzymatic reaction that leads to a compound with lower fluorescence. To assume a pseudo-first order constant, the kinetics experiments were carried-out at 100 nM in Halo probes with a 20-fold excess of protein. In more standard

experimental conditions (1 μM probe and 1.7 eq of protein) the evolution of the fluorescence over time confirms the very fast reaction of **Y-Halo** but with stable fluorescence intensity (Figure S1). Apart from **Y-Halo**, the reaction rates of the probes are slower than that of rhodamine-based HaloTag ligands but they are in the same range or faster than that observed for other reported solvatochromic HaloTag probes[16,18] and for alternative self-labeling protein tags such as SNAP-tag, CLIP-tag and PYP-tag.[4,5,10,12]
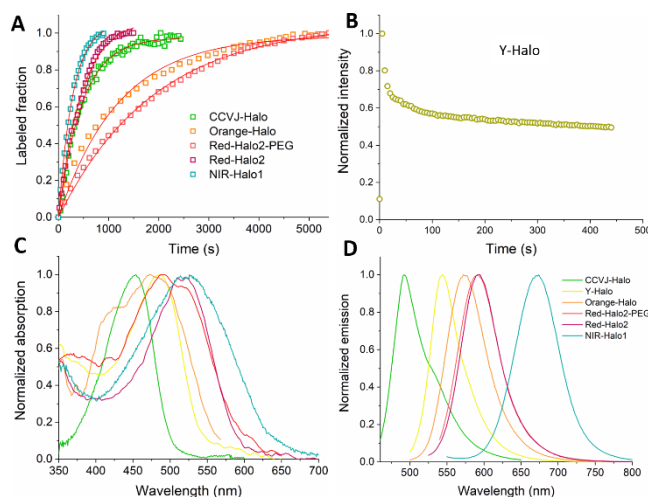

Figure 3. Reaction of the Halo probes with GST-HaloTag.
(A,B) Reaction kinetics of the Halo probes with GST-HT. [dye] = 100 nM, [GST-HT] = 2 μM, T = 298 K. Data was fitted to an exponential rise function (red lines) with the exception of Y-Halo. Normalized absorption (C) and emission (D) of the Halo probes bound to HaloTag. [Dye] = 1 μM [GST-HT] = 1.7 μM.

After reaction with HaloTag, the spectral properties of the bound probes are essentially similar to those in glycerol but with lower fluorogenicities (Table 2). **CCVJ-Halo** and **Y-Halo** display comparable 12 to 15-fold fluorescence activation and while **Red-Halo2-PEG** and **Orange-Halo** perform slightly better, the four new probes have lower fluorescence enhancement factors than their parent compound **Red-Halo2** (156-fold), which stems essentially from lower fluorescence quantum yields. **CCVJ-Halo**, **Y-Halo** and **Orange-Halo** display absorption spectra centered on 458 nm, 489 nm and 487 nm respectively, which allows for an optimal excitation with the 458 and 488 nm Argon laser lines commonly available on microscopes. The **Red-Halo2** derivatives and **NIR-Halo1** can be efficiently excited with the 488 or 514 nm laser lines. Due to their flexible structures that increase the number of available vibrational energy levels, the Halo dyes inherently display broad emission peaks. The more flexible structure **NIR-Halo1** displays the broadest peak, with a FWHM of 68 nm. The emission peaks of **Red-Halo2**, **Red-Halo2-PEG** and **Orange-Halo** have comparable, albeit slightly narrower, breadth (Figure 3C). Although considerable progress has been made in the analysis and spectral deconvolution of multicolor images, these large emission ranges may render their discrimination from other fluorophores more difficult in multiplexed experiments. On the other hand, the green and yellow derivatives, **CCVJ-Halo** and **Y-Halo**, exhibit narrower emission peaks with FWHM of 54 and 50 nm that could make them more easily applicable in multicolor imaging. The new HaloTag fluorogens display promising properties with fluorogenic emissions of varied colors and adequate spectral properties for microscopy. The performance of the probes was next assessed in wash-free live cell imaging with a particular emphasis on the imaging contrast.

Cellular imaging. The probes were first applied to the cellular imaging of live Hela cells transfected with Halo-NLS. This strategy was successfully used in our previous report and the staining of a well-defined region of the cells allows comparing the performance of the various probes by measuring the contrast between the specific nuclear signal and a possible non-specific signal in the cytoplasm.
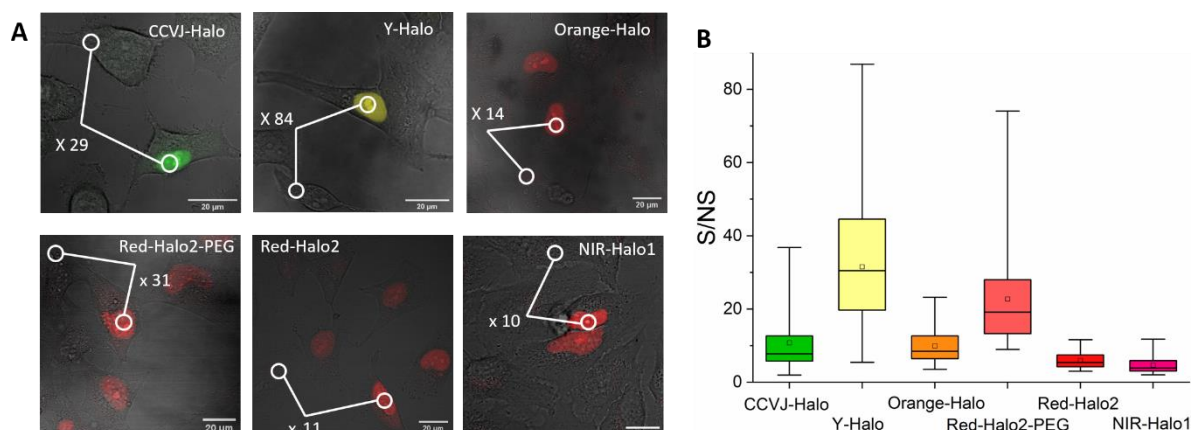
Figure 4. Selectivity and contrast of the Halo probes in cellular imaging.

(A) Live confocal imaging of Hela cells transfected with Halo-NLS plasmid and incubated with 0.5 µM of fluorogenic Halo probe. On each panel is displayed the contrast ratio between the intensity in the nucleus and the non-specific signal measured in the cytoplasm of a non-transfected cell on the same image. λ_{exc} = 514 nm except for CCVJ-Halo (458 nm) and Y-Halo (488 nm). Scale bar : 20 µm (B) Contrast ratio of the specific (S = average intensity in the nucleus) over the non-specific signal (NS = averaged intensity in a cytosolic region of a non-transfected cell). Box and whiskers plot with center lines and squares showing the median and average values for n cells respectively. Box delimits the 25th and 75th percentiles and the whiskers show the max and min values. CCVJ-Halo: n = 64 from four experiments, Y-Halo: n = 43 from two experiments, Red-Halo2-PEG: n = 94 from four experiments, Orange-Halo: n = 91 from three experiments, Red-Halo2: n = 54 from three experiments, NIR-Halo1: n = 72 from four experiments.

The imaging was performed using a similar protocol as for **Red-Halo2**: after transfection the cells were stained with 0.5 µM of Halo probe and were imaged after 30 to 60 minutes without changing the medium or washing the excess dye. After incubation, the cells showed a good viability with no sign of cytotoxicity and all four new probes were successful in selectively staining the nucleus (Figure 3A). To assess the performance of our dye in wash-free imaging protocols, we have compared the specific signal (S) in the nuclei with the non-specific signal (NS) in the cytoplasm of an untransfected cell. Untransfected cells were chosen as reference since transfected cells may exhibit some fluorescence in the cytoplasm due to the reaction of the fluorogen with newly synthesized proteins in the cytoplasm which is not *per se* an off-target binding. The contrast ratio (S/NS) is given on each panel of figure 3A. For a more precise analysis of the probes selectivity, we have calculated the contrast on a larger set of cells and the distribution of the results is given as a box plot on figure 3B. The specific signal (and thus the related contrast) is highly dependent on the transfection level, which causes a large dispersion of the values. Nonetheless, by looking at the average value or at the highest contrast to be expected with a good transfection level, these results clearly show that the newly designed probes with lower lipophilicity **Red-Halo2-PEG** and **Orange-Halo** indeed improve the contrast of the parent compound **Red-Halo2.** Imaging of wild-type Hela cells stained with **Red-Halo2**, **Red-Halo2-PEG** and **Orange-Halo** confirm these observations (Figure S2). Despite the minute structural change between **Red-Halo2** and **Orange-Halo**, the latter yields a cytoplasmic signal 3-fold lower than the former and the effect is even more pronounced with the pegylated derivatives with a 6-fold higher cytoplasmic signal for **Red-Halo2** compared to **Red-Halo2-PEG,** which is well in line with the relative distribution of the S/NS ratios. Interestingly and although they were not specifically designed for this, the **CCVJ-Halo** and **Y-Halo** derivatives also exhibits improved S/NS ratios that reach remarkably high values for the latter. These results stress the difficulty of designing efficient fluorogenic probes and the necessity to balance *in vitro* and cellular properties: a high fluorescence enhancement factor *in vitro* is an important figure of merit for a fluorogenic probe, yet it does not always translate into a high contrast in cellular imaging due to the possibility of off-target fluorogen activation. Here, despite its superior optical properties measured in cuvette, **Red-Halo2** is also the most prone to off-target activation in cells yielding a higher non-specific signal. On the other hand, the new probes exhibit excellent contrast values that are not directly correlated to the relative brightness or fluorescence enhancement values.

In order to take advantage of the increased contrast, we have finally used the palette of HaloTag probes to image of variety of cellular components in addition to the HaloTag-NLS nuclear labeling discussed above (Figure 5 and Figure S3).
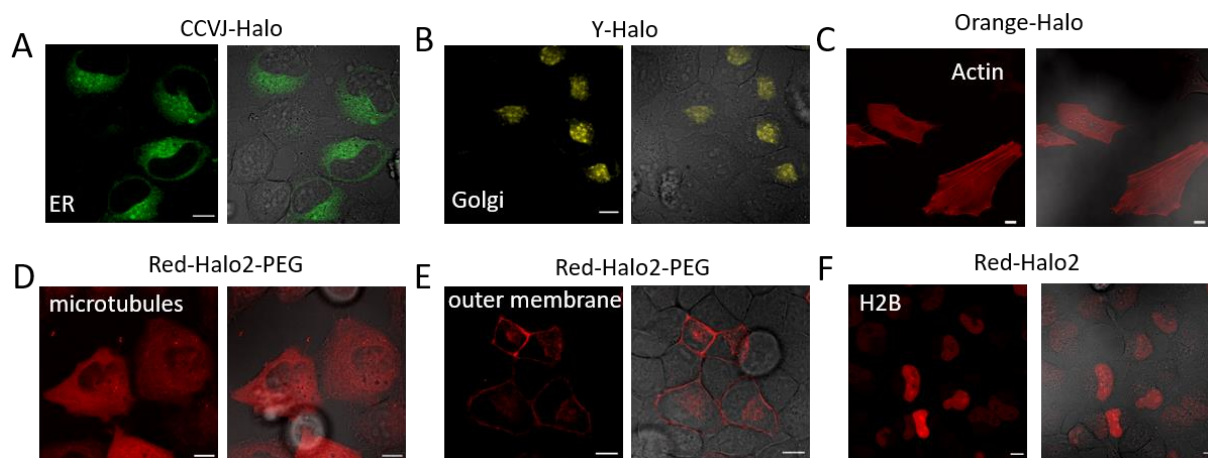

Figure 5. Targeted organelles and proteins imaging.
Live wash-free confocal imaging of Hela cells transfected with either H2B-HaloTag (nucleus), MAP4-HaloTag (microtubules), PGDFR-HaloTag (external membrane), ER-HaloTag (endoplasmic reticulum), HaloTag-Lifeact (actin) or Golgi-HaloTag (Golgi apparatus) and incubated with 0.5 µM of CCVJ-Halo (A), Y-Halo (B) or Orange-Halo (C) Red-Halo2-PEG (D,E) and Red-Halo2 (F). Each panel diplays the fluorescence image (left) and the merged fluorescence and brightfield images (right). Non-transfected cells are visible on the merged images to evidence the selective labeling. λ_{exc} = 514 nm except for CCVJ-Halo (458 nm) and Y-Halo (488 nm) Scale bar: 10 µm.

We have tested the imaging of the ER, the golgi apparatus, histone H2B for a different nuclear staining strategy, microtubules, the outer membrane and actin. In agreement with the results obtained with Halo-NLS, the probes afforded images with good contrast despite the wash-free protocols. The parent compound **Red-Halo2** still proved efficient to image the nucleus or the cytoskeleton using H2B-HaloTag or MAP4-HaloTag, affording contrasted and detailed images thanks to its brightness (Figure 4F and Figure S3). In addition to opening additional possibilities in terms of emission range, the new probes, thanks to their improved selectivity, enabled the imaging of cytoplasmic organelles (Figure 5A&B), which would have been rendered difficult with the original **Red-Halo2**.

Conclusion

The fluorogenic HaloTag probes reported here enrich a palette of hybrid chemogenetic reporters that, combined with the previously reported ones, covers the green to far-red emission range. The newly designed probes offer a remarkable suppression of the non-specific signal enabling no-wash imaging of a variety of intracellular targets with excellent contrast. Recent reports suggest that HaloTag may be mutated to better fit solvatochromic or molecular rotor probes[18,37] Engineering of the HaloTag protein may thus be envisioned in order to improve the association with our fluorogens and to reach higher quantum yields and faster reaction kinetics.

Experimental procedures

Probes synthesis and characterization. Detailed synthetic procedures and chemical analyses are available in the supplementary information.

Photophysical properties with HaloTag. The fluorogenic dyes were dissolved in DMSO at a stock concentration of 0.5 mM. The interaction of the probes with Halotag was assessed by incubating the dye at 1 µM (0.4 µL of stock solution) concentration with 1.7 µM (ca. 6 µL of commercial stock solution) of protein in a 200 µL working volume of pH 7.4 Phosphate buffer (10 mM phosphate with 100 mM NaCl). Fluorescence spectra were recorded

at regular time intervals until completion of the reaction. The different photophysical properties of the protein-bound probes were then measured.

Kinetics study of the labeling reactions. The second-order rate constants of the reactions were calculated by monitoring the fluorescence intensity during the reaction of the probes with a large excess of protein to assume a pseudo first-order kinetics law according to the following procedure.

GST-HT (2 μM) was added to a 50 μL solution of Halo probe (100 nM) in pH 7.4 Phosphate buffer (10 mM Phosphate, 100 mM NaCl). The fluorescence intensity (excitation and emission at the maximum absorption and emission wavelengths of each probe) was then recorded over time until completion of the reaction with a 5 s to 20 s step depending on the probe. The second order rate constants were then calculated according to a previously reported model:[7] the fluorescence was converted to the labeled fraction according to the following equation:

$$Labeled\ fraction = (F-F_0)/(F_{max}-F_0)$$

Where F_{max} and F_0 are the maximum and initial fluorescence intensity respectively. Using Origin 2019 software, the data was fitted to the following equation to calculate the pseudo first-order rate constant k_{obs}:

$$Labeled\ fraction = 1- exp(-k_{obs}t)$$

The second order rate constant k_2 was then obtained by dividing k_{obs} with the protein concentration.

Molecular Biology. Detailed construction of the plasmids used in this study are described in the supplementary information.

Confocal microscopy. Hela cells were grown overnight on 8-well polymer μslides from Ibidi (#1.5 polymer coverslip, tissue culture treated) at 20k to 50k cells/well in 300 μL of MEM culture medium (Gibco) supplemented with 10% fcs, sodium pyruvate and non-essential amino acids. Cells were then transfected with the desired plasmid using Fugene 6 (Promega Corp.) according to the manufacturer's protocol (200 ng of DNA per well with a 3:1 fugene to DNA ratio). After 24 hours, the medium was changed and replaced with DMEM (no phenol red) and the cells were incubated 30-60 minutes with the dyes and imaged live on a Zeiss LSM710 laser scanning confocal microscope equipped with a Plan apochromat 40X/1.4 NA objective. Images were acquired using Zen 2009 software and then processed using ImageJ.

Acknowledgements

Supplementary information

Supplementary figures, materials and methods, chemical synthesis and molecular biology procedures are available in supplementary information.

References

(1) Lavis, L. D.; Raines, R. T. Bright Ideas for Chemical Biology. *ACS Chem. Biol.* **2008**, *3* (3), 142–155.

(2) Day, R. N.; Davidson, M. W. The Fluorescent Protein Palette: Tools for Cellular Imaging. *Chem. Soc. Rev.* **2009**, *38* (10), 2887–2921.

(3) Los, G. V.; Encell, L. P.; McDougall, M. G.; Hartzell, D. D.; Karassina, N.; Zimprich, C.; Wood, M. G.; Learish, R.; Ohana, R. F.; Urh, M.; et al. HaloTag: A Novel Protein Labeling Technology for Cell Imaging and Protein Analysis. *ACS Chem. Biol.* **2008**, *3* (6), 373–382.

(4) Keppler, A.; Gendreizig, S.; Gronemeyer, T.; Pick, H.; Vogel, H.; Johnsson, K. A General Method for the Covalent Labeling of Fusion Proteins with Small Molecules in Vivo. *Nat. Biotechnol.* **2003**, *21* (1), 86–89.

(5) Gautier, A.; Juillerat, A.; Heinis, C.; Corrêa, I. R.; Kindermann, M.; Beaufils, F.; Johnsson, K. An Engineered Protein Tag for Multiprotein Labeling in Living Cells. *Chem. Biol.* **2008**, *15* (2), 128–136.

(6) Hoelzel, C. A.; Zhang, X. Visualizing and Manipulating Biological Processes by Using HaloTag and SNAP-Tag Technologies. *ChemBioChem* **2020**, *21* (14), 1935–1946.

(7) Hori, Y.; Norinobu, T.; Sato, M.; Arita, K.; Shirakawa, M.; Kikuchi, K. Development of Fluorogenic Probes for Quick No-Wash Live-Cell Imaging of Intracellular Proteins. *J. Am. Chem. Soc.* **2013**, *135* (33), 12360–12365.

(8) Plamont, M.-A.; Billon-Denis, E.; Maurin, S.; Gauron, C.; Pimenta, F. M.; Specht, C. G.; Shi, J.; Quérard, J.; Pan, B.; Rossignol, J.; et al. Small Fluorescence-Activating and Absorption-Shifting Tag for Tunable Protein Imaging in Vivo. *Proc. Natl. Acad. Sci.* **2016**, *113* (3), 497–502.

(9) Bruchez, M. P. Dark Dyes-Bright Complexes: Fluorogenic Protein Labeling. *Curr. Opin. Chem. Biol.* **2015**, *27*, 18–23.

(10) Gao, J.; Hori, Y.; Shimomura, T.; Bordy, M.; Hasserodt, J.; Kikuchi, K. Development of Fluorogenic Probes for Rapid High-Contrast Imaging of Transient Nuclear Localization of Sirtuin 3. *ChemBioChem* **2020**, *21* (5), 656–662.

(11) Szent-Gyorgyi, C.; Schmidt, B. A.; Creeger, Y.; Fisher, G. W.; Zakel, K. L.; Adler, S.; Fitzpatrick, J. A. J.; Woolford, C. A.; Yan, Q.; Vasilev, K. V.; et al. Fluorogen-Activating Single-Chain Antibodies for Imaging Cell Surface Proteins. *Nat. Biotechnol.* **2008**, *26* (2), 235–240.

(12) Leng, S.; Qiao, Q.; Miao, L.; Deng, W.; Cui, J.; Xu, Z. A Wash-Free SNAP-Tag Fluorogenic Probe Based on the Additive Effects of Quencher Release and Environmental Sensitivity. *Chem. Commun.* **2017**, *53* (48), 6448–6451.

(13) Yu, W. T.; Wu, T. W.; Huang, C. L.; Chen, I. C.; Tan, K. T. Protein Sensing in Living Cells by Molecular Rotor-Based Fluorescence-Switchable Chemical Probes. *Chem. Sci.* **2016**, *7* (1), 301–307.

(14) Sun, X.; Zhang, A.; Baker, B.; Sun, L.; Howard, A.; Buswell, J.; Maurel, D.; Masharina, A.; Johnsson, K.; Noren, C. J.; et al. Development of SNAP-Tag Fluorogenic Probes for Wash-Free Fluorescence Imaging. *ChemBioChem* **2011**, *12* (14), 2217–2226.

(15) Jung, K. H.; Fares, M.; Grainger, L. S.; Wolstenholme, C. H.; Hou, A.; Liu, Y.; Zhang, X. A SNAP-Tag Fluorogenic Probe Mimicking the Chromophore of the Red Fluorescent Protein Kaede. *Org. Biomol. Chem.* **2019**, *17* (7), 1906–1915.

(16) Liu, Y.; Miao, K.; Dunham, N. P.; Liu, H.; Fares, M.; Boal, A. K.; Li, X.; Zhang, X. The Cation−π Interaction Enables a Halo-Tag Fluorogenic Probe for Fast No-Wash Live Cell Imaging and Gel-Free Protein Quantification. *Biochemistry* **2017**, *56* (11), 1585–1595.

(17) Clark, S. A.; Singh, V.; Vega Mendoza, D.; Margolin, W.; Kool, E. T. Light-Up "Channel Dyes" for Haloalkane-Based Protein Labeling in Vitro and in Bacterial Cells. *Bioconjug. Chem.* **2016**, *27* (12), 2839–2843.

(18) Kang, M.-G.; Lee, H.; Kim, B. H.; Dunbayev, Y.; Seo, J. K.; Lee, C.; Rhee, H.-W. Structure-Guided Synthesis of a Protein-Based Fluorescent Sensor for Alkyl Halides. *Chem. Commun.* **2017**, *53* (66), 9226–9229.

(19) Wang, L.; Tran, M.; D'Este, E.; Roberti, J.; Koch, B.; Xue, L.; Johnsson, K. A General Strategy to Develop Cell Permeable and Fluorogenic Probes for Multicolour Nanoscopy. *Nat. Chem.* **2020**, *12* (2), 165–172.

(20) Grimm, J. B.; English, B. P.; Chen, J.; Slaughter, J. P.; Zhang, Z.; Revyakin, A.; Patel, R.; Macklin, J. J.; Normanno, D.; Singer, R. H.; et al. A General Method to Improve Fluorophores for Live-Cell and Single-Molecule Microscopy. *Nat. Methods* **2015**, *12* (3), 244–250.

(21) Bachollet, S. P. J. T.; Addi, C.; Pietrancosta, N.; Mallet, J.-M.; Dumat, B. Fluorogenic Protein Probes with Red and Near-Infrared Emission for Genetically Targeted Imaging. *Chem. Eur. J.* **2020**, *26* (63), 14467–14473.

(22) Wilhelm, J.; Kühn, S.; Tarnawski, M.; Gotthard, G.; Tünnermann, J.; Tänzer, T.; Karpenko, J.; Mertes, N.; Xue, L.; Uhrig, U.; et al. Kinetic and Structural Characterization of the Self-Labeling Protein Tags HaloTag7, SNAP-Tag, and CLIP-Tag. *Biochemistry* **2021**, *60* (33), 2560–2575.

(23) Encell, L. P. Development of a Dehalogenase-Based Protein Fusion Tag Capable of Rapid, Selective and Covalent Attachment to Customizable Ligands. *Curr. Chem. Genomics* **2012**, *6* (1), 55–71.

(24) Lukinavičius, G.; Reymond, L.; Umezawa, K.; Sallin, O.; D'Este, E.; Göttfert, F.; Ta, H.; Hell, S. W.; Urano, Y.; Johnsson, K. Fluorogenic Probes for Multicolor Imaging in Living Cells. *J. Am. Chem. Soc.* **2016**, *138* (30), 9365–9368.

(25) Grimm, J. B.; Muthusamy, A. K.; Liang, Y.; Brown, T. A.; Lemon, W. C.; Patel, R.; Lu, R.; Macklin, J. J.; Keller, P. J.; Ji, N.; et al. A General Method to Fine-Tune Fluorophores for Live-Cell and in Vivo Imaging. *Nat. Methods* **2017**, *14* (10), 987–994.

(26) Frei, M. S.; Tarnawski, M.; Roberti, J.; Koch, B.; Hiblot, J.; Johnsson, K. HaloTag9 : An Engineered Protein Tag to Improve Fluorophore Performance. *BioRxiv* **2021**, doi: 10.1101/2021.04.01.438024

(27) Fares, M.; Li, Y.; Liu, Y.; Miao, K.; Gao, Z.; Zhai, Y.; Zhang, X. A Molecular Rotor-Based Halo-Tag Ligand Enables a Fluorogenic Proteome Stress Sensor to Detect Protein Misfolding in Mildly Stressed Proteome. *Bioconjug. Chem.* **2018**, *29* (1), 215–224.

(28) Hoche, J.; Schulz, A.; Dietrich, L. M.; Humeniuk, A.; Stolte, M.; Schmidt, D.; Brixner, T.; Würthner, F.; Mitric, R. The Origin of the Solvent Dependence of Fluorescence Quantum Yields in Dipolar Merocyanine Dyes. *Chem. Sci.* **2019**, *10* (48), 11013–11022.

(29) Xie, X.; Zuffo, M.; Teulade-Fichou, M. P.; Granzhan, A. Identification of Optimal Fluorescent Probes for G-Quadruplex Nucleic Acids through Systematic Exploration of Mono- And Distyryl Dye Libraries. *Beilstein J. Org. Chem.* **2019**, *15*, 1872–1889.

(30) Shaya, J.; Collot, M.; Bénailly, F.; Mahmoud, N.; Mély, Y.; Michel, B. Y.; Klymchenko, A. S.; Burger, A. Turn-on Fluorene Push-Pull Probes with High Brightness and Photostability for Visualizing Lipid Order in Biomembranes. *ACS Chem. Biol.* **2017**, *12* (12), 3022–3030.

(31) Péresse, T.; Gautier, A. Next-Generation Fluorogen-Based Reporters and Biosensors for Advanced Bioimaging. *Int. J. Mol. Sci.* **2019**, *20* (24), 6142.

(32) Klymchenko, A. S. Solvatochromic and Fluorogenic Dyes as Environment-Sensitive Probes: Design and Biological Applications. *Acc. Chem. Res.* **2017**, *50* (2), 366–375.

(33) Dumat, B.; Bordeau, G.; Aranda, A. I.; Mahuteau-Betzer, F.; Harfouch, Y. El; Metgé, G.; Charra, F.; Fiorini-Debuisschert, C.; Teulade-Fichou, M.-P. Vinyl-Triphenylamine Dyes, a New Family of Switchable Fluorescent Probes for Targeted Two-Photon Cellular Imaging: From DNA to Protein Labeling. *Org. Biomol. Chem.* **2012**, *10* (30), 6054.

(34) Iwaki, T.; Torigoe, C.; Noji, M.; Nakanishi, M. Antibodies for Fluorescent Molecular Rotors. *Biochemistry* **1993**, *32* (29), 7589–7592.

(35) Goh, W. L.; Lee, M. Y.; Joseph, T. L.; Quah, S. T.; Brown, C. J.; Verma, C.; Brenner, S.; Ghadessy, F. J.; Teo, Y. N. Molecular Rotors as Conditionally Fluorescent Labels for Rapid Detection of Biomolecular Interactions. *J. Am. Chem. Soc.* **2014**, *136* (17), 6159–6162.

(36) Baranov, M. S.; Solntsev, K. M.; Baleeva, N. S.; Mishin, A. S.; Lukyanov, S. A.; Lukyanov, K. A.; Yampolsky, I. V. Red-Shifted Fluorescent Aminated Derivatives of a Conformationally Locked GFP Chromophore. *Chem. Eur. J.* **2014**, *20* (41), 13234–13241.

(37) Miró-vinyals, C.; Stein, A.; Fischer, S.; Ward, T. R.; Deliz Liang, A. HaloTag Engineering for Enhanced Fluorogenicity and Kinetics with a Styrylpyridium Dye. *ChemBioChem* **2021**, *in press*, doi: 10.1002/cbic.202100424.